IEEE Access
Multidisciplinary | Rapid Review | Open Access Journal

Received 23 April 2024, accepted 20 May 2024, date of publication 27 May 2024, date of current version 4 June 2024.

Digital Object Identifier 10.1109/ACCESS.2024.3406260

RESEARCH ARTICLE

SwapTransformer: Highway Overtaking Tactical Planner Model via Imitation Learning on OSHA Dataset

ALIREZA SHAMSOSHOARA, SAFIN B. SALIH, AND PEDRAM AGHAZADEH
Innovation Center of California Volkswagen Group Innovation, Belmont, CA 94002, USA

Corresponding author: Alireza Shamsoshoara (alireza.shamsoshoara@vw.com)

This work was supported by the Volkswagen, Innovation and Engineering Center of California (VW-IECC).

ABSTRACT This paper investigates the high-level decision-making problem in highway scenarios regarding lane changing and over-taking other slower vehicles. In particular, this paper aims to improve the Travel Assist feature for automatic overtaking and lane changes on highways. About 9 million samples including lane images and other dynamic objects are collected in simulation. This data; Overtaking on Simulated HighwAys (OSHA) dataset is released to tackle this challenge. To solve this problem, an architecture called SwapTransformer is designed and implemented as an imitation learning approach on the OSHA dataset. Moreover, auxiliary tasks such as future points and car distance network predictions are proposed to aid the model in better understanding the surrounding environment. The performance of the proposed solution is compared with a multi-layer perceptron (MLP) and multi-head self-attention networks as baselines in a simulation environment. We also demonstrate the performance of the model with and without auxiliary tasks. All models are evaluated based on different metrics such as time to finish each lap, number of overtakes, and speed difference with speed limit. The evaluation shows that the SwapTransformer model outperforms other models in different traffic densities in the inference phase.

INDEX TERMS Autonomous vehicle, dataset, highways, imitation learning, overtaking, transformers.

I. INTRODUCTION

In the past decade, the field of autonomous driving has received lots of attention. Self-driving cars or autonomous vehicles (AV) represent a novelty of artificial intelligence (AI), robotics, computer vision, and sensor technology [1], [2], [3]. Many works focused on end-to-end learning approaches from camera to direct actions such as steering wheel, acceleration, and brake [4], [5], [6]; however, there are many challenges such as lack of interpretability, data efficiency, safety and robustness, generalization, and trade-off between layers that make the end-to-end training less suitable for self-driving cars reliability. On the other hand, modular approaches break down the problem into different tasks such as perception and sensor cognition, motion prediction, high-level and low-level path planner, and motion controller [1], [7], [8]. Self-driving is an intricate problem since it relies on tackling a set of different components such as following traffic laws, precise scene understanding, and performing safe, comfortable, and reliable maneuvers, such as lane changing, parking, etc.

In this study, we narrowed down and targeted the highway overtaking and lane-change problem. The ego vehicle is trying to match the velocity with the speed limit. The goal of overtaking on highways is to stay on the right-most lane unless there is a slow car in front of the ego vehicle. In that case, the ego can use the left lanes to pass other slow vehicles and return to the right-most lane. Figure 1 shows this overtaking task over two vehicles. Proper and on-time lane-change decision-making can help different aspects such as traffic flow, speed maintenance, reducing congestion, and avoiding tailgating [9], [10]. The current technology in commercial vehicles includes a Travel Assist controller that is explained in more detail in section III-A. The Travel Assist

The associate editor coordinating the review of this manuscript and approving it for publication was Wai-Keung Fung.

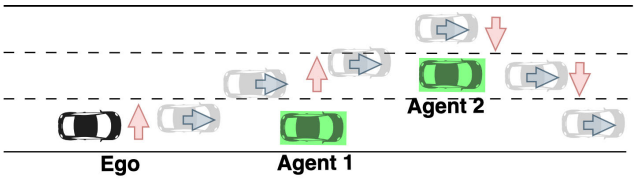

FIGURE 1. An example of an ego vehicle overtaking two agents by making left and right lane changes.

controller is able to automatically move the car from one lane to another lane upon the driver's request. One of the key challenges for this controller is that it still needs the signaling request from the driver and is handled manually. The problem of lane-changing has already been investigated by many approaches such as reinforcement learning [11]. However, usually, reinforcement learning techniques suffer from distributional shifts or gaps between the simulation environment and the real world [12]. Other approaches such as rule-based methods [13], [14] cannot fully handle edge cases in every scenario and situation. Moreover, they are computationally heavy to implement.

In this paper, we present a new AI approach to propose a lane change for the Travel Assist lane change module to perform overtaking and lane changing without human interaction. This AI module considers the safety of the ego based on training data. This paper considers environmental understanding by using a new swapping concept at its core. To have better generalizations, future points and car network predictions are proposed as auxiliary tasks. These auxiliary tasks are not involved in decision-making for the lane changes at the inference time; however, training these two subtasks improves performance at inference time. The model is tested successfully in a simulation environment.

The contributions of this study are as follows:

- OSHA Dataset: we are releasing a highway lane change dataset that is collected using the SimPilot simulation. This dataset is gathered based on the realistic behavior of vehicles in a simulation environment. About 9 million samples are collected as raw data and processed for the training aspect. OSHA dataset is available as a public resource [15] (Link).
- SwapTransformer: This model provides lane change predictions in highway scenarios. The swapping feature in the transformer is the key to better understanding the context and correlation between all agents including ego vehicle and other dynamic objects through features and time simultaneously.
- Auxiliary tasks: Our model solves secondary tasks such as future point and car network prediction sharing the same base with main tasks. We showed that while the output of auxiliary tasks does not explicitly affect the behavior of the ego vehicle, it helps during the training to better understand the dynamics of surrounding vehicles and road structure.
- Benchmarks: We made an excessive comparison for the proposed model and other baselines at inference time to evaluate metrics such as time-to-finish the scene, number of lane changes, and overtakes.

The rest of this paper is organized as follows. Section II discusses the related works in imitation learning. The Travel Assist controller, data collection, simulation environment, rule-based driver, and dataset are explained in sections III-A and III-B. Sections IV-A and IV-B propose the idea of SwapTransformer and how auxiliary tasks affect the training phase for better generalization and scene understanding. Evaluation is discussed in detail in section V by explaining simulation and training setups and assessing models. In the end, the conclusion is discussed in section VI. More low-level details about the implementation are mentioned in the Appendix C.

II. RELATED WORKS

This section focuses on imitation learning approaches regarding lane-changing and overtaking scenarios and related technical approaches.

Imitation learning is one of the earliest and most successful methods for Autonomous Driving tasks. Authors in [16], [17], and [18] have used different variations of Imitation Learning to solve overtaking or lane changing specifically.

Authors in [19] showed that using a long short-term memory (LSTM) module for Lane Change (LC) prediction achieves a significant improvement in both adaptive cruise control (ACC) and cooperative adaptive cruise control. In another work [18], the authors used a convolutional neural network (CNN) to show that this network is capable of learning the expert policy excellently.

In [16], the proposed approach solved discretionary lane changes considering different driving styles. They utilized CNNs to extract the ego and its surrounding vehicles' driving operational picture. Since their context movable objects are present, they also extract three traffic factors: speed gain, safety, and tolerance. These extracted features will be concatenated with the driving operational pictures and fed to an MLP. Spatio-temporal CNNs are used in [20], where the available data of eight vehicles (ego and seven surrounding vehicles in front and on both sides), stacked over time, is the input.

Authors in [21] have developed lane-changing behavior detection using residual neural networks. Their proposed network solves this classification problem more accurately than the approaches combining support vector machines, principal component analysis, or vanilla CNN network, while trained end-to-end without a specific lane detection module using ResNet [22]. They also point out that this data is in time sequences, so in the future, using modules like recurrent neural networks (RNN) or LSTMs will help analyze the entire data sequence. Furthermore, in [23], authors have classified the state-of-the-art deep learning approaches for vehicle behavior prediction, including lane change detection for ego or surrounding vehicles. This review further proves the usage of RNNs and CNNs in lane change behavior prediction.

With the extensive use of attention architecture in large language models and their proven capabilities in learning long-term dependencies and fusing features, authors in [24] and [25] used a combination of imitation learning and attention modules for autonomous driving tasks. In both of the aforementioned works the networks are inspired by Vision Transformers [26] since they use images from cameras to predict waypoints.

The popularity of transformer models [27] shows why they are also an excellent choice for AD tasks [28]. Reference [29] uses an attention-based LSTM model on top of a C4.5 [30] decision tree to predict the lane change intention and execution. While in this work, the attention mechanism automatically extracts the critical information and learns the relationship between the hidden layers, in [28], the trajectory prediction of other vehicles is solved by combining language models and trajectory prediction. Instead of predicting independent features for each agent, authors devised an approach employing attention to combine features across different dimensions (such as road elements, agent interactions, and time steps).

In other works such as [31], the authors proposed Lane Transformer to perform a lane changes trajectory prediction. The idea was to use attention-based blocks to replace the Graph Convolutional Networks (GCNs). This idea resulted in better performance compared to state-of-the-art models with fewer model parameters and less size in memory making the approach more suitable for edge devices and TensortRT. The authors compared their approach with Argoverse baseline and LaneGCN on different offline metrics such as min-Average Displacement Error (min-ADE), min- Final Displacement Error (min-FDE), and Miss Rate (MR).

The authors in [32] considered the application of automated driving systems (ADSs) for trajectory and maneuver predictions. The authors claimed that in environments like highways where the ego car interacts with lots of uncertainties from other vehicles, it is beneficial to have a multimodal prediction for intentions and trajectories to rank different outcomes. They used a transformer-based model as a backbone for feature learning and next, they fed the extracted representation to different heads for trajectory and maneuver generation.

In another work [33], the authors tried to address the lack of interpretability in long-term prediction for lane change behaviors on highways. They introduced an approach called the Lane-Change Large Language Model (LC-LLM) to provide an explanation and reasoning for each lane change that the ego vehicle is making on highways. The authors used open-source Llama-2-7b-chat [34] as a base-foundation model to fine-tune their processed data. The proposed approach showed how the capabilities of reasoning and self-explanation can improve the reasoning and performance for lane change prediction on different metrics and performances such as root-mean-squared-error of lateral and longitudinal trajectory.

As discussed in this section, although many works have focused on attention-based networks, there is a lack of focus on the combination of features and temporal information for the ego vehicle concerning decision-making. This motivated us to propose the idea of SwapTransformer and auxiliary task definition.

III. SYSTEM MODEL

A. TRAVEL-ASSIST CONTROLLER

In this study, we assumed that the ego vehicle is an electric vehicle equipped with the Travel Assist feature that includes three key components [35], [36]: The first component is ACC which keeps and adjusts the speed based on what the driver set in the car and tries to consider traffic flow to avoid a collision with a vehicle in front. If a vehicle in front slows down, the ACC will slow down to keep a safe distance and once it is safe, it will accelerate to the speed that was set by the driver. The second component is lane-keeping assist (LKA) which uses cameras to detect the lane and keep the car in the lane. If the driver is not signaling, and the car drifts away from the center of the lane, LKA steers the vehicle and controls the car to the center of the lane. Finally, the last component is the lane change assist; once the driver triggers the signal, this module monitors the surrounding lanes for other vehicles. If it is safe, the car gradually moves to the requested lane by the driver; otherwise, it will reject the request.

Vehicles with Travel Assist utilize cameras and Radar. Specifically, Travel Assist can steer, accelerate, and decelerate the ego vehicle. The input for the lane change assist has three options, keep the current lane, change to the left lane, and change to the right lane. Figure 1 shows those triggers for the ego vehicle. Travel Assist controller is used by the rule-based algorithm for data collection. Moreover, the trained model interacts with the Travel Assist controller at the inference time to control the ego vehicle. Travel Assist controller consists of seven different states 1) None, 2) Instantiated, 3) Ready-to-change, 4) Start-movement, 5) Interrupted, 6) Success, and 7) Failed. The controller receives the lane change command in the None state and follows other corresponding states.

Figure 2 shows different states and phases of the Travel Assist controller. The controller starts in the *None* state and upon receiving the lane change action, it goes to the *instantiated* state. In this state, the ego car starts signaling for a specific amount of time. Next, it goes to *Ready-to-change* state which the travel assist checks for safety. If it is safe to change, the ego car will start changing lanes (*start the lateral movement*), otherwise, it will go to *Interrupt* followed by *Fail* states and then back to the *None* state. In simulation, Sumo has another sanity check for the lane change; while this does not exist in reality. In the last condition, the Travel Assist controller checks if lane change occurred or not, and based on that states of *Success* or *Fail* are defined.

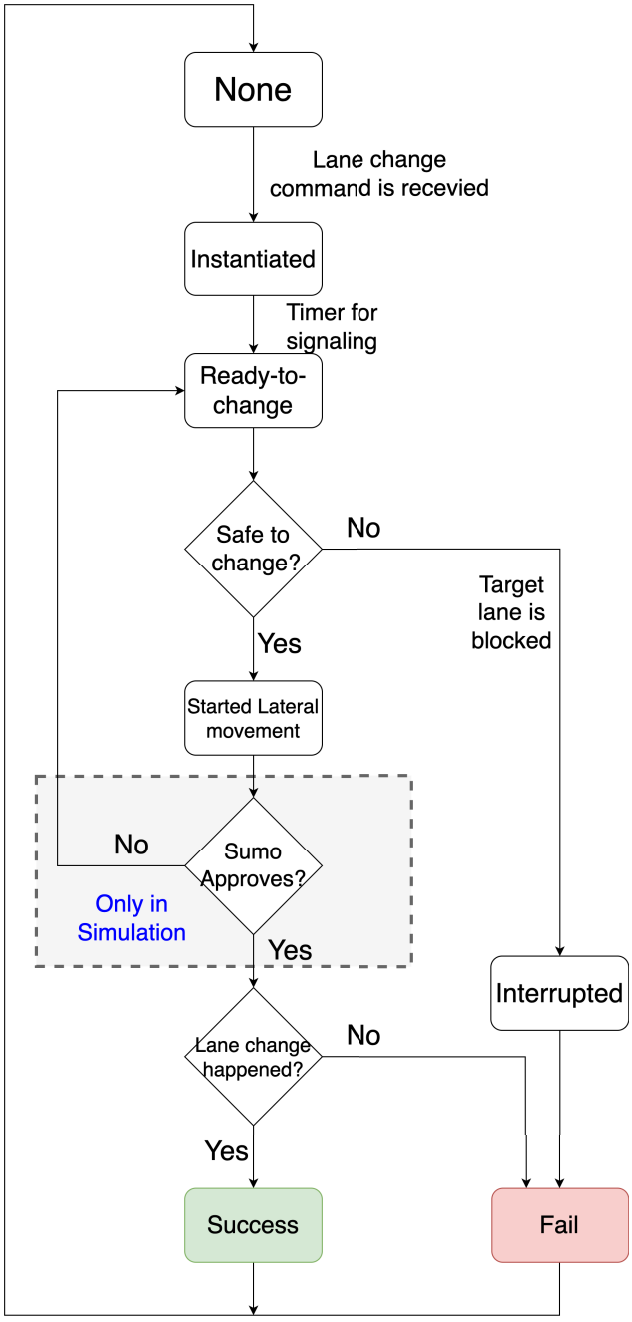

FIGURE 2. Travel Assist flowchart including different states.

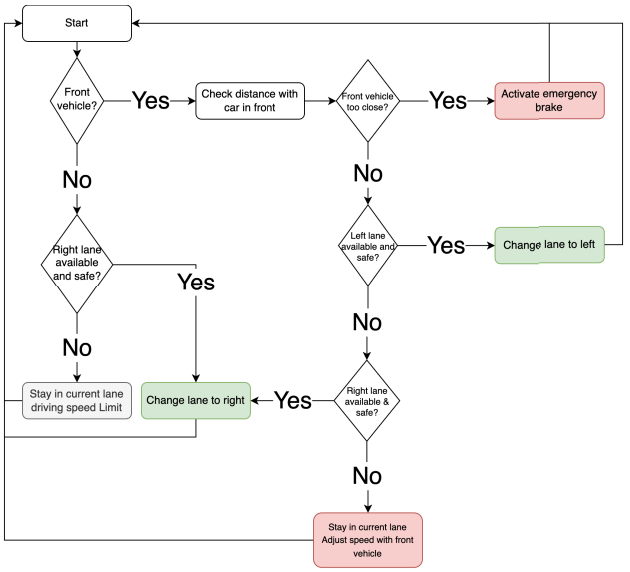

FIGURE 3. Rule-based algorithm flowchart.

B. DATA COLLECTION

This section discusses the importance of data generation in regards to imitation learning used in Section IV. First, the simulation environment SimPilot is introduced, the rule-based algorithm is described, and lastly, the features of raw and processed data are detailed.

1) SIMPILOT: SIMULATION ENVIRONMENT

SimPilot is the name of the driving simulation which is built in-house based on the Unity engine [37]. Unity provides the required graphics and physics for the ego vehicle and other dynamic and static objects. Sumo controls the traffic behavior in SimPilot in the background [38]. The SimPilot platform provides different cities such as Berlin and San Francisco, and training and evaluation scenes for highways. In this paper, highway scenes are used. SimPilot provides different types of sensors and observations based on real-world hardware and implementation. SimPilot is able to communicate with Python through a software called MLAgent [39]. Using MLAgent, our AI model is able to control the Travel Assist module and hence control the ego vehicle. Specifically in this approach, observations are received through MLAgent and fed to the model, and then the output of the model is sent back to the SimPilot to control the ego vehicle.

SimPilot communicates with the Python interface with a frequency of 50 Hz which is equal to 20ms in simulation timestep. The simulation environment provides object list data for 20 vehicles around the ego within the vicinity of 100m.

2) RULE-BASED DRIVER

We developed a simple rule-based driver to control the ego for data collection purposes. Despite the fact that Sumo is capable of controlling ego, we opted to develop our custom ego driver. The primary motivation for developing this rule-based driver was to retrieve the lane change commands, as Sumo could not. In our approach, we considered the six vehicles surrounding the ego to decide on a lane change. These six vehicles are the vehicles in front and behind the ego in the current lane and the adjacent lanes if they exist. The state of each vehicle can be represented as (x, y, v, ID), where (x, y) is the relative position to ego, V is velocity, and ID is the lane ID. A lane change will happen only if all four conditions of *Safety*, *Speed gain*, *Availability*, and *Controller acceptance* are met (definitions can be found in Appendix A).

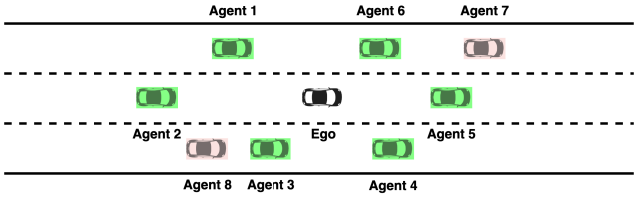

FIGURE 4. Observation space for the proposed Rule-based algorithm.

The flowchart in Figure 3 represents the general policy of the rule-based driver. An overtake is defined as two lane changes, where ego will make a lane change, pass the vehicle in front, and then if there is enough space to get back to the original lane, another lane change will occur. As previously mentioned, the controller has safety features to avoid collisions. However, the safety of each lane change is also checked by considering the current state of the available lane. This improves the quality of lane changes with a higher success rate. Figure 4 shows how the ego vehicle perceives the simulation environment (more detailed explanation can be found at Appendix A).

C. OSHA DATASET: RAW AND PROCESSED DATA

OSHA dataset is created by a combination of rule-based driver and SimPilot simulation for training and validation purposes. In this study, we collected raw data by utilizing the rule-based driver as an expert driver to collect sensor and lane information. To match the data requirement with vehicle hardware and sensors, only lane ID segmentation is collected as vision data. Other information is collected as ego vehicle data and object list. Different traffic densities vary from 5 to 35 vehicles per kilometer are used for data collection. The environment is seeded and after each episode, the ego car is located in a random lane and location on the scene. Three types of speed behavior as *slow*, *normal*, and *fast* are considered for other dynamic objects. The scene is partitioned into different segments with different speed limits. Data samples are explained in detail in Appendix B.

Ego vehicle data is a tuple of $\langle v, s, L_{ID}, l, r, c\rangle$ where $v \in R^+ \cup \{0\}$ is the ego velocity. s is the speed limit associated with that part of the road that ego currently is driving with pre-defined values as integers in $[\frac{m}{s}]$ unit. L_{ID} is an integer value for the current lane ID of ego. $l,\ r \in \{0, 1\}$ are boolean values indicating if left or right lanes are available, respectively. ego location $(x,\ y)$ are also collected in meters defined in a global coordinate system. ego location is used for the auxiliary task of the future position prediction. Also, all rule-based lane-change commands (c), for the current, left, and right lanes are collected at each time step.

On the other hand, simulation provides information about other vehicles as well. This information for each vehicle is a tuple of $\langle v_k, x_k, y_k, L_{ID_k}, m_k\rangle$ where $v_k \in R^+ \cup \{0\}$ is the velocity for vehicle k. $x_k, y_k \in R$ are the positions for vehicle k defined in a local coordinate where the ego is at the origin $(0,\ 0)$. The length of k^{th} vehicle is defined as m_k where $m_k \in R, \forall k \in [1, 20]$. During the processing phase, the future positions are computed for each time step B1. Since SwapTransformer in section IV requires future positions, speed, and lane change commands at each time step; 2.5 seconds (5 points each 500ms apart) of the future data from the recorded samples are extracted and linked to the corresponding timestep.

TABLE 1. Dataset features for raw and processed data.

Description	Raw Data	Processed data
Number of pickle files	900	1
Pickle file size (single)	34.1 MB	61 GB
Images size	5.7 MB (episode)	35 GB
Total number of samples	8,970,692	8,206,442
Lane change commands	5,147	69,119
Left lane commands	2,648	35,859
Right lane commands	2,499	33,260
Transition commands	0	1,468,115
Number of episodes	900	834
Samples per episode	10,000	9,839 (Average)
Speed limit values	$\{30,\ 40, \ldots,\ 80\}(\frac{km}{h})$	$\{30,\ 40, \ldots,\ 80\}(\frac{km}{h})$
ego speed range	$[0,\ 79.92](\frac{km}{h})$	$[0,\ 79.92](\frac{km}{h})$

Since the number of lane changes to left and right lanes is noticeably smaller than the number of commands to stay in the current lane commands, the dataset becomes imbalanced. Before pre-processing the raw data, on average 20 lane changes occur in each episode of collected data with 20,000 steps. Hence, another pre-processing is performed to artificially add augmented lane changes to the original data. A new class called *Transition* is defined to highlight the lane-changing phase between two lanes and it reduces the effect of the imbalanced classes. In addition to the new class, the dataset is augmented to include more lane change commands. Since it takes about 20 steps for the controller to process the lane change command and start the maneuver, those steps are augmented as artificial lane changes.

Figure 5 shows how the pre-processing phase adds those new lane changes and the transition class to the dataset. Before doing any pre-processing, only a single left lane change is detected in Figure 5a; however, after adding the new class; *Transition*, and artificial lane changes, the dataset becomes more balanced. This is illustrated in Figure 5b.

Table 1 shows some details about the dataset used in this paper. More specifically, we show some differences between raw and processed data regarding the number of lane changes, the number of samples, and episodes. Speed limit and ego speed values are common between raw and processed data. The dataset is available here [15] (Link) with more details and features. More information about the OSHA dataset is available in Appendix B.

The unique aspect of the OSHA dataset is that the controller is adapted based on real-world production vehicles, distinguishing it from other datasets or simulations. This dataset is designed for those focusing on high-level decision-making, where actions are interpreted through a motion

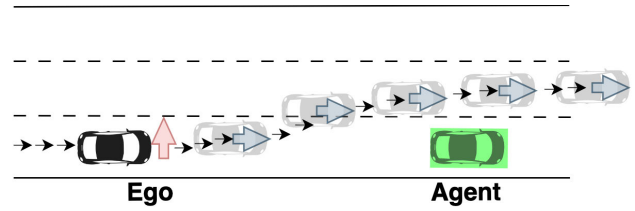

(a) Raw data for lane changes.

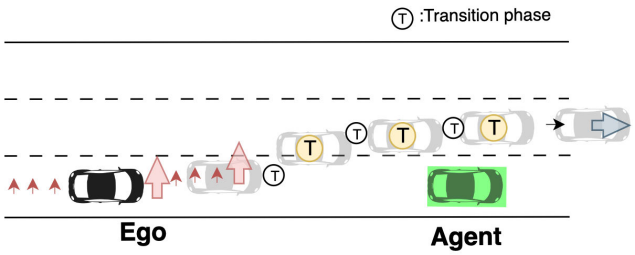

(b) Processed data for lane changes.

FIGURE 5. Difference between before pre-processing and after pre-processing on lane changes.

controller. The dataset can also be applied as a motion forecasting task since it contains positions of ego and all agents surrounding that in each episode. Our focus is solely on high-level decision-making from a bird-eye-view perspective. While other motion forecasting datasets from Waymo [40], Lyft [41], and Argoverse [42] that focus on urban scenarios, ours offers a unique advantage by providing both high-level and low-level actions in diverse highway scenarios.

IV. PROPOSED APPROACH

Our model utilizes two inputs; 1) Lane ID segmentation images, which identify and segment road lanes and demonstrate road curvature. 2) Object lists containing detailed information about the ego vehicle and surrounding cars. For the ego vehicle, this includes current velocity, lane ID, lane change status, lane availability, and speed limit. For other cars, it comprises velocity, relative position to the ego vehicle (x, y), lane ID, and vehicle length. These inputs are stacked in sequences of data, with a history length of five seconds, enabling the model to learn spatio-temporal patterns.

Next, lane ID images are encoded using a CNN encoder network (ResNet 18 [22]), and object list information is processed through an attention-based module. This module employs self-attention across features and time, correlating them to capture fine-grained details and meaningful connections in the object list data.

The model also employs auxiliary tasks (dashed lines in Figure 6) to improve feature representation and gauge performance. One auxiliary task predicts the ego vehicle's future positions, while another, based on the attention module, generates a car graph representing vehicle distances using edges and nodes of a complete graph.

In the main tasks (solid lines in Figure 6), we use the output from the attention module. These outputs are then directed into two distinct MLPs: one is responsible for predicting future lane changes, while the other predicts future velocity. Future predictions serve to enhance our understanding of upcoming dynamic states. Specifically, we predict five future lane changes and velocities; however, the Travel Assist controller only takes the first point to influence the vehicle's behavior [43].

$$\mathcal{L}_{\text{CE, LC}} = -\frac{1}{N}\sum_{i=1}^{N} p_i \log(\hat{f}_i) \tag{1}$$

As shown in Equation (1), $\mathcal{L}_{\text{CE, LC}}$ assesses the model's ability to predict lane changes, including right lane change, left lane change, maintaining the same lane, and transitioning. It penalizes discrepancies between predicted probabilities (p_i) and actual outcomes (f_i) using cross-entropy loss.

$$\mathcal{L}_{\text{MSE, V}} = \frac{1}{N}\sum_{i=1}^{N}(v_i - \hat{v}_i)^2 \tag{2}$$

In addition to the lane change prediction, (2) assesses the model's ability to predict future vehicle velocities. It quantifies the accuracy of velocity predictions by comparing predicted velocities ($\hat{v}_i$) to actual velocities (v_i) for each sample. This loss is defined based on the mean squared error (MSE).

A. SWAPTRANSFORMER

SwapTransformer addresses limitations in traditional self-attention mechanisms [27], particularly in scenarios with object lists containing temporal sequences. By employing a "swapping" mechanism (Figure 7) within a single transformer encoder, SwapTransformer integrates both time and object list dimensions, enhancing the model's ability to correlate temporal and feature information.

Initially, we take input data, in the form of an object list (detailed in the first paragraph of Section IV), and process them through an embedding layer while also incorporating positional encoding. These inputs consist of a batch of data points where each data point is represented as a 3D tensor comprising time information, an arbitrary embedded dimension, and features sourced from the object list. SwapTransformer operates on the input data tensor $\mathbf{X}$, where $\mathbf{X}$ has shape $T \times N \times D$ (Figure 7), representing temporal, object, and embedding dimensions. Within each layer of the transformer encoder, swapping involves transposing dimensions of $\mathbf{X}$ and feeding it to the next encoder.

Iteratively, passing the inputs through each transformer encoder constructs multiple layers of abstraction, enabling the model to learn complex representations of the input data and make accurate predictions.

B. AUXILIARY TASKS

Solving auxiliary tasks in deep learning is a valuable strategy that offers several advantages. First, it acts as a form of

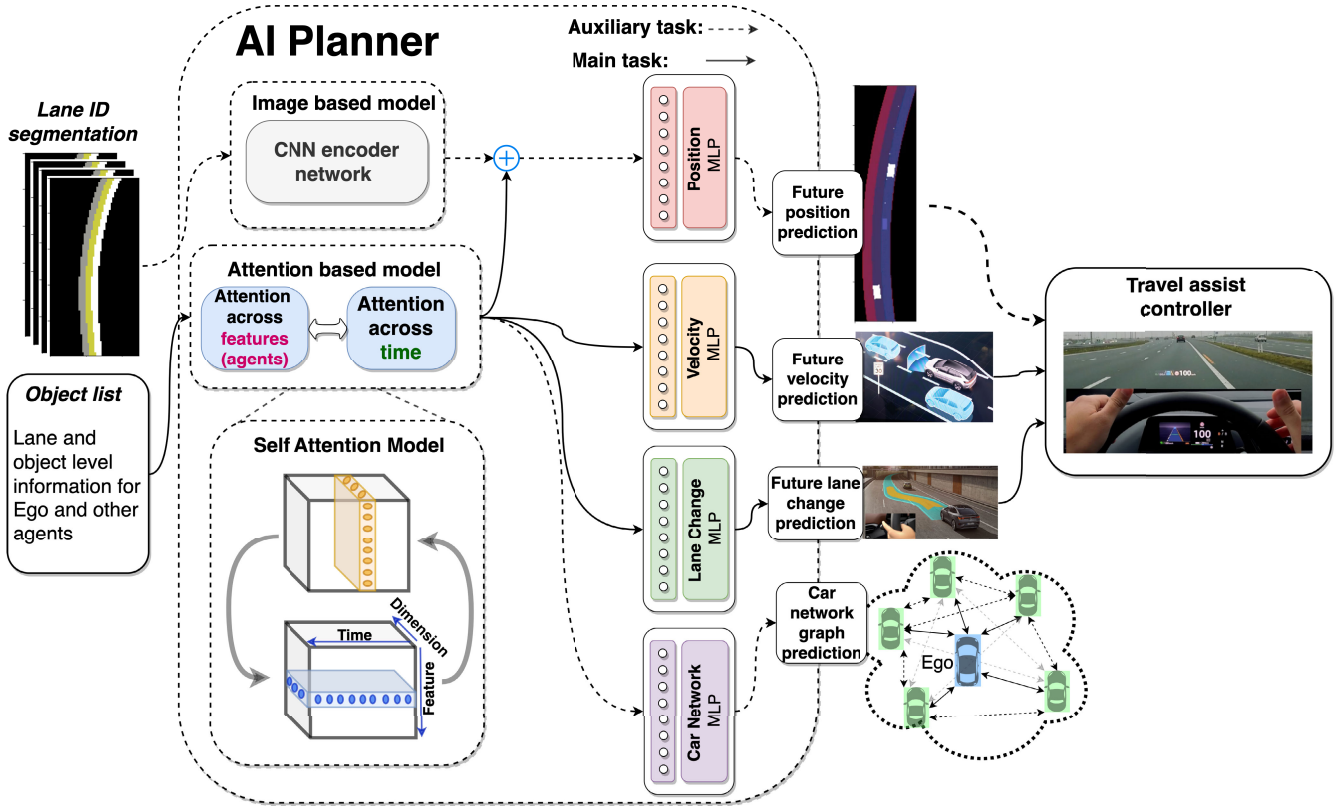

FIGURE 6. SwapTransformer architecture to interact with Travel Assist controller.

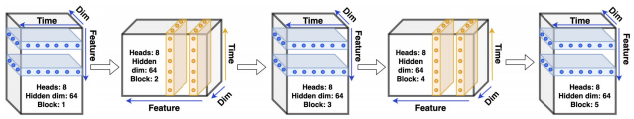

FIGURE 7. Time and feature swapping in SwapTransformer: Considering an example of SwapTransformer with a depth of five attention encoders; Initially, SwapTransformer applies the attention on the time domain on the 3D tensor input and next, it transposes the output and applies attention on the feature domain. This process iterates, allowing the model to capture temporal and feature relationships.

regularization, preventing overfitting and enhancing model generalization. Second, it promotes feature learning, allowing the model to extract meaningful representations from the data. Addressing auxiliary tasks is not a novel approach in the realm of deep learning; it has been employed in various subdomains [44], [45], [46].

1) FUTURE POSE PREDICTION

We propose two auxiliary tasks, the first one is predicting the future positions of the ego vehicle, which aids in comprehending future dynamics. Our model predicts the (C_x, C_y) coordinates of the control points of a Bezier curve, followed by fitting the Bezier curve. Bezier curves are commonly used in trajectory planning for efficient vehicle motion modeling and prediction. Their versatility and controllability make them a preferred choice for representing and generating smooth paths for autonomous vehicles [47]. By leveraging Bezier curves, our auxiliary task improves future pose predictions.

$$\begin{aligned} B(t) = {} & (1-t)^4 \cdot C_0 + 4(1-t)^3 \cdot t \cdot C_1 \\ & + 6(1-t)^2 \cdot t^2 \cdot C_2 + 4(1-t) \cdot t^3 \cdot C_3 \\ & + t^4 \cdot C_4, \quad 0 \le t \le 1 \end{aligned} \tag{3}$$

In the context of the Bezier curve (3), the parameter t represents the parametric value or parameterization along the curve that ranges from 0 to 1. Typically, t is used to interpolate between control points and generate the smooth path described by the Bezier curve. In this case, we omit the C_0 point because it starts at $(0, 0)$, and our model focuses on predicting the subsequent control points (C_x, C_y) that define the curve's shape and trajectory. We selected the quartic Bezier curve because of its ability to capture more complex and subtle curve shapes compared to lower-order Bezier curves, such as quadratic or cubic Bezier curves. We evaluated lower-order Bezier curves and the quartic curves yielded the lowest error compared to the ground truth curves. The loss function used for future pose prediction as the auxiliary task is:

$$\mathcal{L}_{BZ}(p,\ \hat{p}) = \frac{1}{N}\sum_{i=1}^{N}(||p_i - \hat{p}_i||_2^2 \cdot w_i), \tag{4}$$

where $\mathcal{L}_{BZ}$ is the weighted loss value between the prediction $\hat{p}_i$ and ground truth p_i for a batch with n samples.

$w_i = e^{\frac{1}{K-i}} - 1$ is the weighted vector applied to different points of the predictions to have better results on farther points. K represents an arbitrary constant value for the number of points in the line.

2) CAR NETWORK PREDICTION

Our secondary auxiliary task aids in comprehending the spatial relations and awareness among all vehicles within a given scene. We generate distance matrices that include all vehicles, including the ego vehicle as:

$$D = \begin{bmatrix} 0 & d_{0,1} & d_{0,2} & \cdots & d_{0,19} & d_{0,\text{ego}} \\ d_{1,0} & 0 & d_{1,2} & \cdots & d_{1,29} & d_{1,\text{ego}} \\ d_{2,0} & d_{2,1} & 0 & \cdots & d_{2,19} & d_{2,\text{ego}} \\ \vdots & \vdots & \vdots & \ddots & \vdots & \vdots \\ d_{19,0} & d_{19,1} & d_{19,2} & \cdots & 0 & d_{19,\text{ego}} \\ d_{\text{ego},0} & d_{\text{ego},1} & d_{\text{ego},2} & \cdots & d_{\text{ego},19} & 0 \end{bmatrix}, \quad (5)$$

where $d_{i,j} \in \mathbb{R}^+ \cup \{0\}$ is the Euclidean distance between any pair of vehicles i and j, including the ego and other objects. We should also mention that we mask out (m_{vehicle}) distances when no vehicles are present in the scene to account for empty scenarios in the loss function. In this loss (6), $D \in \mathbb{R}^{N \times N}$ represents the ground truth (actual) distances between vehicles, and $\hat{D}$ represents the distances predicted by our model.

$$\mathcal{L}_{\text{MSE, CN}} = \frac{1}{N} \sum_{i=1}^{N} \left((D_i - \hat{D}_i)^2 \cdot m_{\text{vehicle}} \right) \quad (6)$$

To ensure our model effectively learns all relevant features, we must back-propagate through this total loss (7). The components of this total loss include cross-entropy loss for various lane change classes, regression on velocity differences, regression on losses related to Bezier curves, and finally, regression on the Car Network loss.

$$\mathcal{L}_{\text{total}} = \mathcal{L}_{\text{CE, LC}} + \mathcal{L}_{\text{MSE, V}} + \mathcal{L}_{\text{BZ}} + \mathcal{L}_{\text{MSE, CN}} \quad (7)$$

V. EVALUATION

A. SIMULATION SETUP

After completing data collection and training of the SwapTransformer, we conducted an evaluation in a simulated environment to compare the set of models. During this evaluation phase, each model undergoes inference for 50 episodes in an unseen environment 11b for a maximum of 20,000 steps (equivalent to 400 seconds) or until completing one lap around the track, whichever happens first. Additionally, our assessment encompassed three distinct traffic scenarios, categorized as follows: low, medium, and high density with 5, 15, and 25 vehicles per km on the road, respectively (More details can be found at Appendix D).

B. TRAINING SETUP

Training is performed on a local cloud instance with a learning rate $\alpha = 0.0001$, batch size of 256 on 8 GPUs (Nvidia A100 - 80GB memory) in a distributed data-parallel manner. Adam [48] is used as an optimizer during training alongside ResNet18 as the feature extractor for lane ID segmentation. All five models in table 2 were trained for 300 epochs taking approximately two days to train each model. More details about the training are available in Section VII-D. The purpose of training five models with the selected features is to compare them and see the effect of each module on different performance metrics in the next section.

C. INFERENCE AND RESULTS

Table 2 reports the performance evaluation for the SwapTransformer. In this table, "MLP" and "Transformer only" are considered as the baseline for the proposed problem. "Transformer + Aux." and "Transformer + Swap" are two intermediate models before the proposed solution ("SwapTransformer (Transformer + Swap + Aux.)". Unlike other datasets and tools such as WOMD [49] and Waymax [50] which are defined based on the motion forecasting domain, our problem is meant for a combination of high-level decision-making along with low-level trajectory prediction. Hence, comparing the baselines in two different domains is out of the scope of this paper.

The first column of table 2 reports how each trained model is behaving at velocity prediction during inference time. A model with better speed following with respect to the speed limit has a lower metric. In the speed difference column of table 2, our model outperforms other models in low and medium traffic densities. Based on the content of table 2 SwapTransformer model outperforms all the other models in all traffic densities by finishing the loop fastest in all traffic scenarios.

The last column of table 2 shows the left overtake ratio in a highway environment. The average number of vehicles overtaken by each model is maximum with the SwapTransformer model in medium- and high-density traffic scenarios. It is noted that, in medium-traffic densities, all models exhibit a higher frequency of overtaking maneuvers as opposed to high-traffic densities. This disparity can be rationalized by the congestion in high-density traffic, which leaves limited opportunities for overtaking. Subsequently, after conducting comparisons among various models during the inference phase, we proceeded to execute the SwapTransformer model with auxiliary tasks to demonstrate its interaction with the SimPilot environment, as illustrated in Figure 8.

The combination of auxiliary tasks and dimension-swapping exhibits synergistic effects, enhancing the model's performance by leveraging both strategies concurrently. However, when individually trained—either with Transformer + Auxiliary or Transformer + Swap—both models exhibit a tendency to underfit within the 300-epoch computational budget. In the swap transformer, we 'swap' dimensions between the time horizon and features. If trained longer, Transformer+Aux or Transformer+Swap by themselves would outpace the Transformer in evaluation. Hence, the Swap mechanism and auxiliary tasks are complementary in

TABLE 2. Comparison between SwapTransformer (ours) and other baselines on different metrics.

Metrics	1) Speed difference (m/s) ↓			2) Time to finish (s) ↓			3) Left overtake ratio ↑		
Traffic	Low	Med	High	Low	Med	High	Low	Med	High
MLP (Baseline)	3.19 ± 0.7	4.16 ± 0.98	4.37 ± 0.77	181.24 ± 9.2	192.02 ± 7.78	193.59 ± 7.39	0.04	0.02	0.06
Transformer only	2.11 ± 0.46	2.81 ± 1.28	$\mathbf{3}.45 \pm 1.66$	170.27 ± 4.23	174.07 ± 3.45	179.69 ± 7.18	0.12	0.28	0.24
Transformer + Aux.	2.25 ± 0.35	2.9 ± 0.75	4.19 ± 1.44	171.84 ± 3.36	178.8 ± 8.08	193.05 ± 11.78	**0.2**	0.16	0.12
Transformer + Swap	2.73 ± 0.99	3.26 ± 0.94	4.2 ± 0.98	174.34 ± 5.82	182.32 ± 7.85	195.11 ± 12.3	0.1	0.18	0.1
Transformer + Swap + Aux. (Ours)	$\mathbf{2}.09 \pm 0.5$	$\mathbf{2}.45 \pm 1.2$	3.55 ± 1.97	$\mathbf{168}.7 \pm 1.99$	$\mathbf{169}.97 \pm 2.47$	$\mathbf{176}.93 \pm 9.32$	0.16	**0.38**	**0.3**

FIGURE 8. Frames of decision-making with the SwapTransformer at the inference time.

terms of faster convergence during training because of the additional signals they provide for each other [51]. Different inference demos are available in [52] and [53] (YouTube) and (Github). It can be observed that during lane changes, the behavior of future points is more aligned with the new decision to land on a new lane on the highway. Interestingly, one can see the future positions drifting towards another lane right before a lane change command is sent. This further proves the effect of auxiliary tasks on the performance of main tasks (Figure 8).

A notable challenge arises in overtaking as there is no precise metric for directly comparing different models. This challenge emerges from the inherent variability in decision-making within similar scenarios, wherein models may exhibit slight variations in their lane change decisions over a few sequential steps. Even minor divergences in decision-making (e.g., deciding on a right lane change instead of keeping the current lane) can result in substantial differences in the environmental states of different models, hence comparing the models to the rule-based driver on a step-wise basis does not accurately reflect the performance of models.

Regarding comparison with other similar works such as Wayformer or Multipath++ [54], [55] models and approaches, most of those methods are focused on motion forecasting using end-to-end methods. Our contribution to this work is to propose an approach for imitation learning especially behavioral cloning rather than focusing on motion forecasting. Moreover, we are considering the modular autonomous driving stacks where high-level decision-making is the interface between the model and the low-level controller. Hence, this is one of the first hybrid approaches in the planning domain making it infeasible to compare it with other approaches. One of the benefits of using a modular architecture is that we can apply it to real vehicles equipped with the Travel Assist controller. Thus, our approach and dataset are unique to others.

VI. CONCLUSION

In this research paper, we tackled the problem of lane changing and overtaking on highways. We have introduced an AI approach using imitation learning called SwapTransformer. To train this model, 9 million frames containing overtakes with different traffic densities are collected in the simulation. This data is released as the OSHA dataset which is currently accessible by the public. SwapTransformer leverages dimension transposition, temporal and feature-based attention mechanisms, and auxiliary tasks like predicting future positions and distance matrices. In performance evaluations against MLP and transformer baseline models, SwapTransformer consistently outperformed them across diverse traffic densities, as evidenced by lap completion time, speed deviation from the limit, and overtaking score metrics, showcasing its robust generalization capabilities.

VII. FUTURE WORKS

This is an ongoing project and based on the progress in the simulation platform next steps are split as:

- The first step is the implementation in reality and testing of the SwapTransformer on real-world highways. This phase of implementation in SimPilot is proved as a proof-of-concept. There already exists real-world data from highway scenarios collected by vehicles equipped with the Travel Assist module. However, a fleet of cars is already ready to collect more data for fine-tuning the SwapTransformer.
- Another future direction involves bringing the navigation information as an additional input to the SwapTransformer for entering and exiting highways. The aim of this task is to have more intelligent lane changing and overtaking considering the navigation commands.
- Motion forecasting of other dynamic vehicles plays a vital role in the planner module. Currently, a motion forecasting model is trained and available as an independent AI model to predict the future trajectories and positions of other vehicles on highways. We believe that feeding these predicted outputs as an additional input to the SwapTransformer will help the tactical planner

to make wiser and safer lane change and overtaking decisions.

REPRODUCIBILITY

We are committed to promoting transparency and reproducibility in our research. To facilitate the replication of our results, we provide comprehensive information about the code, data, and methods used in this study. Appendix provides more information about OSHA dataset and also the source code used for data processing, model training, and evaluation is available in the supplementary materials of this paper.

APPENDIX

A. RULE-BASED ALGORITHM

The rule-based driver is a simple physical model based on a set of rules and numerical thresholds that are determined by experiments and previous work on physical models controlling the vehicle [56], [56], [57]. As explained in the paper, the rule-based algorithm has different components for decision-making. The precise definition of each component for a lane change can be described as:

- Safety: This includes the time to collision with the vehicle in front of ego in the current lane, the vehicle in front of the destination lane, and behind ego in both lanes. Plus, the distance between the ego and vehicles in front and behind it in both lanes should be greater than or equal to the safe distances defined.
- Speed gain: The purpose of a lane change in our approach is to drive faster and match the speed limit. Given all the available information about surrounding vehicles, estimate the speed at which ego will move after the lane change happens and compare it with the estimated speed of staying in the current lane. This condition is met if the ego can drive faster after a lane change. Or if there is an available right lane where ego can drive as fast in it, a right lane change will happen.
- Availability: Not only should there be a lane available next to the ego for a lane change to happen, but there should also be enough space for the ego to move to that lane. In other words, another vehicle should not be parallel to ego in the destination lane.
- Controller acceptance: On top of all the previous three conditions required for a reasonable lane change, our controller might reject a lane change command sent due to a sudden lane change or acceleration of surrounding vehicles.

The six vehicles in the ego's current lane and (possibly) adjacent left and right lanes (as shown in Figure 4) will be used to make a decision. For each vehicle we use the $\langle v_k, x_k, y_k, L_{ID_k}, m_k \rangle$ where $v_k \in R^+ \cup \{0\}$ is the velocity for vehicle k. $x_k, y_k \in R$ are the positions for vehicle k defined in a local coordinate where the ego is at the origin $(0,\ 0)$. The length of k^{th} vehicle is defined as m_k where $m_k \in R, \forall k \in [1, 20]$. The relative position of each vehicle can be found easily and we can label them as current-front, current-rear, left-front, left-rear, right-front, and right-rear.

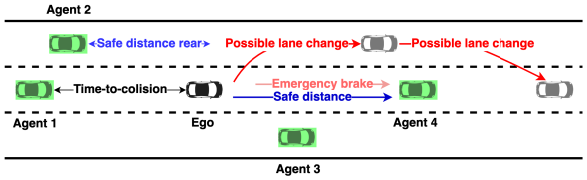

FIGURE 9. Rule-based safety metrics.

For simplicity, other agents available in the field of view of ego are not considered. In Figure 4, agents 7 and 8 are not observed by the rule-based driver.

To have a reasonable lane change, we also consider the speed of the vehicles in the destination lane. This also includes the distance to vehicles in the rear and front and the time distance (also known as time of collision). Also, Figure 9 shows how an overtake will consist of two lane changes in a short period, as well as showing the emergency brake distance and safe distance that will be kept with the vehicle in front at all times. The safe distance in the rear is part of our additional requirement for a lane change. Even though the Travel Assist controller has internal safety conditions to perform a lane change we wanted to make sure that model learns the best behaviors possible.

It is worth noting that the rule-based algorithm was implemented based on many fine-tuning and tweaks on many parameters to cover a simple highway scenario. However, it needs lots of effort to have a rule-based approach for all different scenarios. The rule-based algorithm has limited access only to the vehicles adjacent to the ego (front, rear, left, and right) whereas the SwapTransformer has access to all the vehicles visible and can potentially understand more complex dynamic behaviors. The main reason for developing the rule-based approach is to have an automated way to generate ground truth data. As pointed out in Section VII (future works), the rule-based will be replaced by human drivers to collect realistic data.

B. DATASET

1) FUTURE POSITION

As explained in the paper, those future points are needed as ground truth for the auxiliary task purpose. Future position processing and transformation from global to local coordinate system are shown in:

$$(x_{t+i},\ y_{t+i})_{\text{local}} = \begin{bmatrix} \cos(\phi_t) & \sin(\phi_t) \\ -\sin(\phi_t) & \cos(\phi_t) \end{bmatrix} \begin{bmatrix} x_{t+i} - x_t \\ y_{t+i} - y_t \end{bmatrix}_{\text{global}} \quad \forall 1 \leq i \leq 5, \tag{8}$$

where x_{t+i} and y_{t+i} are the future processed local positions for t^{th} sample in the dataset in the vector format. In this study, five future locations are considered for prediction. Hence the vector has five future positions such as (x_{t+i} and y_{t+i}) $= \{(x_{t+1}, y_{t+1}), (x_{t+2}, y_{t+2}), \ldots, (x_{t+5}, y_{t+5})\}$. ϕ_t is the orientation for the ego car at time stamp t in the global coordinate system. The second matrix is used to calculate the

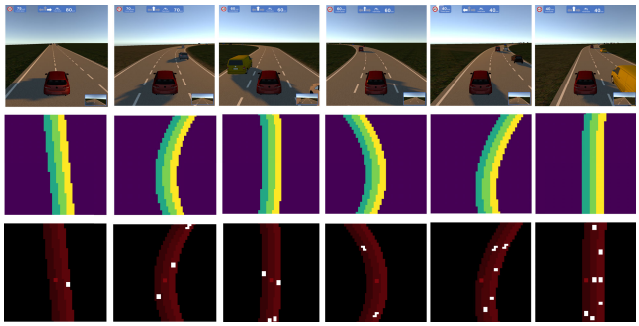

FIGURE 10. A few samples from the dataset [15] (Link).

relative distance between the future and current location of the ego in the global coordinate system.

2) DATA PRUNING

During the pre-processing phase, some all samples that result in collisions are removed from the dataset. This means if a collision happens between the ego and other vehicles at any time, the pre-processing phase trims that episode to avoid having those samples in the training dataset. In general, a collision may happen when other vehicles hit the ego vehicle, due to a sudden lane change. In addition, since the model is predicting five future points which are 2.5 seconds in the future, the end of all episodes is cut to have meaningful data for training. This results in 8,206,442 samples of data after pre-processing out of 8,970,692 raw samples. Also, a few new features are added to the raw dataset for the sake of training. These new features are future positions, future velocity, future lane change commands, and a matrix of distances between each pair of vehicles including the ego and others.

Figure 10 illustrates a few samples of the dataset. The first row shows the GUI sample of the surrounding environment and the second row shows the road curvature based on different lane IDs mapped to the segmentation of the drivable area. The third row displays how other dynamic objects(vehicles) are rasterized to the lane ID segmentation image with respect to the ego vehicle location. The data collected and shared in this dataset is one channel with a dimension of 50 pixels in width by 100 pixels in height. The resolution for the image is set as 0.5 meters per pixel. The ego vehicle is located at a fixed location in each image. The ego is horizontally at the center and vertically, it has 10 pixels offset below the center. The image data are stored in PNG format and ego and other vehicles' features and information are stored in pickled pandas data frame format.

C. MODEL DETAILS

Algorithm 1 outlines a procedure for processing batches of data using a set of Transformer Encoders denoted as ψ. It operates on individual elements X_i in a dataset batch, each of which is represented as a tuple $X_i = [t_i,\ d_i,\ f_i]$, where t_i is the historical and temporal information, d_i is an arbitrary embedded dimension with respect to data, and f_i is the feature inputs with respect to ego vehicle and object list. The algorithm begins by applying Positional Encoding (PE) to the input X_i. Then, it iteratively applies the Transformer Encoders from the set ψ to the encoded input $X_{\text{i, encoded}}$, with alternating transformations based on whether the index of the encoder is even or odd.

ALGORITHM 1 SwapTransformer

for *batch* in Dataset **do**
  Let $X_i \in$ batch;
  $X_i = [t_i,\ d_i,\ f_i]$;
  Let ψ be a set of Transformer Encoders;
  $X_{\text{i, encoded}} = PE(X_i)$;
  for n in [1,2,... $|\psi|$] **do**
    if n mod 2 == 0 **then**
      H = $\psi_n(H^T)$;
    else
      H = $\psi_n(H)$;

D. TRAINING AND EVALUATION

In more detail, Figures 11a and 11b demonstrate the map and road structure for training and inference scenes respectively. As illustrated, the inference scene has a completely different shape so we can better evaluate the generalization of the proposed model. Especially, the curvature of the evaluation scene was set to be different than the training scene while designing the evaluation scene.

During the initial stages of model design and training, hyperparameter tuning was performed on the naive transformer without auxiliary loss or the swapping feature to optimize performance. Various versions of EfficientNet [58] (b2 and b6) and ResNet (18, 50) were considered, along with a custom vision encoder. ResNet18 was chosen for its similar performance to other models with lower computational costs. Hyperparameter sweeps using WandB [59] were conducted to determine optimal values for learning rate, scheduler, optimizer, batch size, activation layers, and regularization. Moreover, all models used the same seed at the training time for weight initialization.

Figure 8 in section V-C demonstrated six samples in six different scenarios with different traffic behaviors. The prediction of future points is shown as yellow points as an auxiliary one. Velocity action is directly applied to the Travel Assist controller and the ego speed can be shown at the top left corner of each sample. The lane change command is also illustrated as signaling on the ego and as an arrow in the top layer.

During the evaluation time, the same seed is used for all evaluations between different models. This brings fairness to the comparison. The randomness that applied at the inference and evaluation time accounted for traffic behavior like density, placement, and velocity of other agents. All these randomnesses were defined based on some average and standard deviation (same mean and std for all of them in different situations).

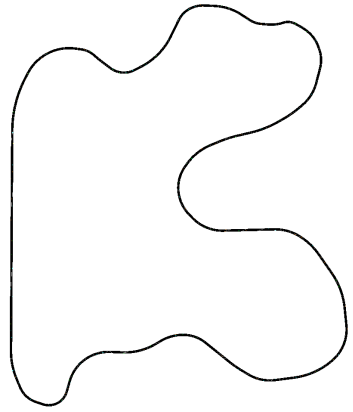

(a) Training scene map.

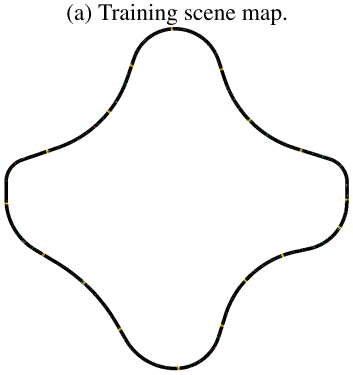

(b) Inference scene map.

FIGURE 11. Difference between training and inference scenes.

ACKNOWLEDGMENT

The authors would like to thank the Simulation team (VW-Innovation Center of Europe) for supporting this research regarding the SimPilot environment. *(Alireza Shamsoshoara, Safin B. Salih, and Pedram Aghazadeh contributed equally to this work.)*

REFERENCES

[1] S. Grigorescu, B. Trasnea, T. Cocias, and G. Macesanu, "A survey of deep learning techniques for autonomous driving," *J. Field Robot.*, vol. 37, no. 3, pp. 362–386, Apr. 2020.

[2] Y. Xiao, F. Codevilla, A. Gurram, O. Urfalioglu, and A. M. López, "Multimodal end-to-end autonomous driving," *IEEE Trans. Intell. Transp. Syst.*, vol. 23, no. 1, pp. 537–547, Jan. 2022.

[3] É. Zablocki, H. Ben-Younes, P. Pérez, and M. Cord, "Explainability of deep vision-based autonomous driving systems: Review and challenges," *Int. J. Comput. Vis.*, vol. 130, no. 10, pp. 2425–2452, Oct. 2022.

[4] M. Bojarski, D. Del Testa, D. Dworakowski, B. Firner, B. Flepp, P. Goyal, L. D. Jackel, M. Monfort, U. Müller, J. Zhang, X. Zhang, J. Zhao, and K. Zieba, "End to end learning for self-driving cars," 2016, *arXiv:1604.07316*.

[5] J. Kim and C. Park, "End-to-end ego lane estimation based on sequential transfer learning for self-driving cars," in *Proc. IEEE Conf. Comput. Vis. Pattern Recognit. Workshops*, Jul. 2017, pp. 30–38.

[6] Z. Yang, Y. Zhang, J. Yu, J. Cai, and J. Luo, "End-to-end multi-modal multi-task vehicle control for self-driving cars with visual perceptions," in *Proc. 24th Int. Conf. Pattern Recognit. (ICPR)*, Aug. 2018, pp. 2289–2294.

[7] S. Atakishiyev, M. Salameh, H. Yao, and R. Goebel, "Explainable artificial intelligence for autonomous driving: A comprehensive overview and field guide for future research directions," 2021, *arXiv:2112.11561*.

[8] S. Teng, X. Hu, P. Deng, B. Li, Y. Li, D. Yang, Y. Ai, L. Li, Z. Xuanyuan, F. Zhu, and L. Chen, "Motion planning for autonomous driving: The state of the art and future perspectives," 2023, *arXiv:2303.09824*.

[9] S. Ulbrich and M. Maurer, "Towards tactical lane change behavior planning for automated vehicles," in *Proc. IEEE 18th Int. Conf. Intell. Transp. Syst.*, Sep. 2015, pp. 989–995.

[10] J. Nilsson and J. Sjöberg, "Strategic decision making for automated driving on two-lane, one way roads using model predictive control," in *Proc. IEEE Intell. Vehicles Symp. (IV)*, Jun. 2013, pp. 1253–1258.

[11] M. P. Ronecker and Y. Zhu, "Deep Q-network based decision making for autonomous driving," in *Proc. 3rd Int. Conf. Robot. Autom. Sci. (ICRAS)*, Jun. 2019, pp. 154–160.

[12] S. Aradi, "Survey of deep reinforcement learning for motion planning of autonomous vehicles," *IEEE Trans. Intell. Transp. Syst.*, vol. 23, no. 2, pp. 740–759, Feb. 2022.

[13] P. Lin, E. Javanmardi, Y. Tao, V. Chauhan, J. Nakazato, and M. Tsukada, "Time-to-collision-aware lane-change strategy based on potential field and cubic polynomial for autonomous vehicles," in *Proc. IEEE Intell. Vehicles Symp.*, Jun. 2023, pp. 1–6.

[14] H. Scheidel, H. Asadi, T. Bellmann, A. Seefried, S. Mohamed, and S. Nahavandi, "A novel approach of a deep reinforcement learning based motion cueing algorithm for vehicle driving simulation," 2023, *arXiv:2304.07600*.

[15] A. Shamsoshoara, S. Salih, and P. Aghazadeh, "Osha dataset," Volkswagen Innov. Eng. Center California, Belmont, CA, USA, Tech. Rep., 2023, doi: 10.21227/ha78-f960.

[16] Y. Zhang, Q. Xu, J. Wang, K. Wu, Z. Zheng, and K. Lu, "A learning-based discretionary lane-change decision-making model with driving style awareness," *IEEE Trans. Intell. Transp. Syst.*, vol. 24, no. 1, pp. 68–78, Jan. 2023.

[17] M. Shin and J. Kim, "Adversarial imitation learning via random search in lane change decision-making," 2021, *arXiv:2109.05197*.

[18] S. A. Pashaki, A. Nahvi, A. Ahmadi, S. Tavakoli, S. Naeemi, and S. H. Shamchi, "Autonomous slalom maneuver based on expert drivers' behavior using convolutional neural network," in *Proc. 10th RSI Int. Conf. Robot. Mechatronics (ICRoM)*, Nov. 2022, pp. 335–340.

[19] A. Nejadhossein Qasemabadi, S. Mozaffari, M. Rezaei, M. Ahmadi, and S. Alirezaee, "A novel model for driver lane change prediction in cooperative adaptive cruise control systems," 2023, *arXiv:2305.01096*.

[20] B. Mersch, T. Höllen, K. Zhao, C. Stachniss, and R. Roscher, "Maneuver-based trajectory prediction for self-driving cars using spatio-temporal convolutional networks," in *Proc. IEEE/RSJ Int. Conf. Intell. Robots Syst. (IROS)*, Sep. 2021, pp. 4888–4895.

[21] Z. Wei, C. Wang, P. Hao, and M. J. Barth, "Vision-based lane-changing behavior detection using deep residual neural network," in *Proc. IEEE Intell. Transp. Syst. Conf. (ITSC)*, Oct. 2019, pp. 3108–3113.

[22] K. He, X. Zhang, S. Ren, and J. Sun, "Deep residual learning for image recognition," in *Proc. IEEE Conf. Comput. Vis. Pattern Recognit.*, Jun. 2015, pp. 770–778.

[23] S. Mozaffari, O. Y. Al-Jarrah, M. Dianati, P. Jennings, and A. Mouzakitis, "Deep learning-based vehicle behavior prediction for autonomous driving applications: A review," *IEEE Trans. Intell. Transp. Syst.*, vol. 23, no. 1, pp. 33–47, Jan. 2022.

[24] R. Zhu, P. Huang, E. Ohn-Bar, and V. Saligrama, "Learning to drive anywhere," 2023, *arXiv:2309.12295*.

[25] J. Du, Y. Zhao, and H. Cheng, "Target-point attention transformer: A novel trajectory predict network for end-to-end autonomous driving," 2023, *arXiv:2308.01496*.

[26] A. Dosovitskiy, L. Beyer, A. Kolesnikov, D. Weissenborn, X. Zhai, T. Unterthiner, M. Dehghani, M. Minderer, G. Heigold, S. Gelly, J. Uszkoreit, and N. Houlsby, "An image is worth 16×16 words: Transformers for image recognition at scale," 2021, *arXiv:2010.11929*.

[27] A. Vaswani, N. Shazeer, N. Parmar, J. Uszkoreit, L. Jones, A. N. Gomez, Ł. Kaiser, and I. Polosukhin, "Attention is all you need," in *Proc. Adv. Neural Inf. Process. Syst.*, vol. 30, 2017, pp. 1–10.

[28] J. Ngiam, V. Vasudevan, B. Caine, Z. Zhang, H.-T. L. Chiang, J. Ling, R. Roelofs, A. Bewley, C. Liu, and A. Venugopal, "Scene transformer: A unified architecture for predicting future trajectories of multiple agents," in *Proc. Int. Conf. Learn. Represent.*, 2021, pp. 1–25.

[29] K. Liang, J. Wang, and A. Bhalerao, "Lane change classification and prediction with action recognition networks," in *Proc. Eur. Conf. Comput. Vis.*, 2022, pp. 617–632.

[30] J. R. Quinlan, *C4.5: Programs for Machine Learning*. San Francisco, CA, USA: Morgan Kaufmann, 1993. [Online]. Available: http://portal.acm.org/citation.cfm?id=152181

[31] Z. Wang, J. Guo, Z. Hu, H. Zhang, J. Zhang, and J. Pu, "Lane transformer: A high-efficiency trajectory prediction model," *IEEE Open J. Intell. Transp. Syst.*, vol. 4, pp. 2–13, 2023.
[32] S. Mozaffari, M. A. Sormoli, K. Koufos, and M. Dianati, "Multimodal manoeuvre and trajectory prediction for automated driving on highways using transformer networks," *IEEE Robot. Autom. Lett.*, vol. 8, no. 10, pp. 6123–6130, Oct. 2023.
[33] M. Peng, X. Guo, X. Chen, M. Zhu, K. Chen, X. Wang, and Y. Wang, "LC-LLM: Explainable lane-change intention and trajectory predictions with large language models," 2024, *arXiv:2403.18344*.
[34] H. Touvron, L. Martin, K. Stone, P. Albert, A. Almahairi, Y. Babaei, N. Bashlykov, S. Batra, P. Bhargava, and S. Bhosale, "Llama2: Open foundation and fine-tuned chat models," 2023, *arXiv:2307.09288*.
[35] Volkswagen. (2021). *Travel Assist | Volkswagen Newsroom*. Accessed: Aug. 22, 2023. [Online]. Available: https://www.volkswagen-newsroom.com/en/travel-assist-15398
[36] M. T. Wolf and J. W. Burdick, "Artificial potential functions for highway driving with collision avoidance," in *Proc. IEEE Int. Conf. Robot. Autom.*, Sep. 2008, pp. 3731–3736.
[37] J. K. Haas, "A history of the unity game engine," *Diss. Worcester Polytech. Inst.*, vol. 483, p. 484, Mar. 2014.
[38] M. Behrisch, L. Bieker, J. Erdmann, and D. Krajzewicz, "SUMO—Simulation of urban mobility: An overview," in *Proc. 3rd Int. Conf. Adv. Syst. Simul.*, 2011, pp. 1–6.
[39] A. Juliani, V.-P. Berges, E. Teng, A. Cohen, J. Harper, C. Elion, C. Goy, Y. Gao, H. Henry, M. Mattar, and D. Lange, "Unity: A general platform for intelligent agents," 2018, *arXiv:1809.02627*.
[40] S. Ettinger, S. Cheng, B. Caine, C. Liu, H. Zhao, S. Pradhan, Y. Chai, B. Sapp, C. Qi, Y. Zhou, Z. Yang, A. Chouard, P. Sun, J. Ngiam, V. Vasudevan, A. McCauley, J. Shlens, and D. Anguelov, "Large scale interactive motion forecasting for autonomous driving : The Waymo open motion dataset," in *Proc. IEEE/CVF Int. Conf. Comput. Vis. (ICCV)*, Oct. 2021, pp. 9690–9699.
[41] B. Wilson, W. Qi, T. Agarwal, J. Lambert, J. Singh, S. Khandelwal, B. Pan, R. Kumar, A. Hartnett, J. Kaesemodel Pontes, D. Ramanan, P. Carr, and J. Hays, "Argoverse 2: Next generation datasets for self-driving perception and forecasting," 2023, *arXiv:2301.00493*.
[42] J. Houston, G. Zuidhof, L. Bergamini, Y. Ye, L. Chen, A. Jain, S. Omari, V. Iglovikov, and P. Ondruska, "One thousand and one hours: Self-driving motion prediction dataset," in *Proc. Conf. Robot Learn.*, Nov. 2021, pp. 409–418.
[43] A. Hu, G. Corrado, N. Griffiths, Z. Murez, C. Gurau, H. Yeo, A. Kendall, R. Cipolla, and J. Shotton, "Model-based imitation learning for urban driving," in *Proc. Adv. Neural Inf. Process. Syst.*, vol. 35, 2022, pp. 20703–20716.
[44] K. He, X. Chen, S. Xie, Y. Li, P. Dollár, and R. Girshick, "Masked autoencoders are scalable vision learners," in *Proc. IEEE/CVF Conf. Comput. Vis. Pattern Recognit. (CVPR)*, Jun. 2022, pp. 15979–15988.
[45] Y. Chen, P. Praveen, M. Priyantha, K. Muelling, and J. Dolan, "Learning on-road visual control for self-driving vehicles with auxiliary tasks," in *Proc. IEEE Winter Conf. Appl. Comput. Vis. (WACV)*, Jan. 2019, pp. 331–338.
[46] A. Mehta, A. Subramanian, and A. Subramanian, "Learning end-to-end autonomous driving using guided auxiliary supervision," in *Proc. 11th Indian Conf. Comput. Vis., Graph. Image Process.*, Dec. 2018, pp. 1–8.
[47] J.-W. Choi, R. Curry, and G. Elkaim, "Path planning based on Bézier curve for autonomous ground vehicles," in *Proc. Adv. Elect. Electron. Eng.-IAENG Special Ed. World Congr. Eng. Comput. Sci.*, 2008, pp. 158–166.
[48] D. P. Kingma and J. Ba, "Adam: A method for stochastic optimization," 2014, *arXiv:1412.6980*.
[49] K. Chen, R. Ge, H. Qiu, R. Ai-Rfou, C. R. Qi, X. Zhou, Z. Yang, S. Ettinger, P. Sun, Z. Leng, M. Baniodeh, I. Bogun, W. Wang, M. Tan, and D. Anguelov, "WOMD-LiDAR: Raw sensor dataset benchmark for motion forecasting," 2023, *arXiv:2304.03834*.
[50] C. Gulino, J. Fu, W. Luo, G. Tucker, E. Bronstein, Y. Lu, J. Harb, X. Pan, Y. Wang, and X. Chen, "Waymax: An accelerated, data-driven simulator for large-scale autonomous driving research," in *Proc. Adv. Neural Inf. Process. Syst.*, vol. 36, 2024, pp. 1–13.
[51] S. Ruder, "An overview of multi-task learning in deep neural networks," 2017, *arXiv:1706.05098*.
[52] VWIECCResearch. (2023). *Demo Inference on SwapTransformer*. Accessed: Feb. 15, 2024. [Online]. Available: https://youtu.be/gNKsLh06eAg?si=w2V5SNR1NZkN2nqC
[53] V. IECCResearch. (2023). *SwapTransformer: Highway Overtaking Tactical Planner Model Via Imitation Learning on OSHA Dataset*. [Online]. Available: https://github.com/VWIECCResearch/Swaptransformer
[54] N. Nayakanti, R. Al-Rfou, A. Zhou, K. Goel, K. S. Refaat, and B. Sapp, "Wayformer: Motion forecasting via simple & efficient attention networks," in *Proc. IEEE Int. Conf. Robot. Autom. (ICRA)*, May 2023, pp. 2980–2987.
[55] B. Varadarajan, A. Hefny, A. Srivastava, K. S. Refaat, N. Nayakanti, A. Cornman, K. Chen, B. Douillard, C. P. Lam, D. Anguelov, and B. Sapp, "MultiPath++: Efficient information fusion and trajectory aggregation for behavior prediction," in *Proc. Int. Conf. Robot. Autom. (ICRA)*, May 2022, pp. 7814–7821.
[56] C. Xu, W. Zhao, J. Liu, C. Wang, and C. Lv, "An integrated decision-making framework for highway autonomous driving using combined learning and rule-based algorithm," *IEEE Trans. Veh. Technol.*, vol. 71, no. 4, pp. 3621–3632, Apr. 2022.
[57] Y. Li, L. Li, D. Ni, and W. Wang, "Hierarchical automatic lane-changing motion planning: From self-optimum to local-optimum," 2021, *arXiv:2108.05711*.
[58] M. Tan and Q. Le, "EfficientNet: Rethinking model scaling for convolutional neural networks," in *Proc. Int. Conf. Mach. Learn.*, 2019, pp. 6105–6114.
[59] L. Biewald. (2020). *Experiment Tracking With Weights and Biases*. [Online]. Available: https://www.wandb.com/

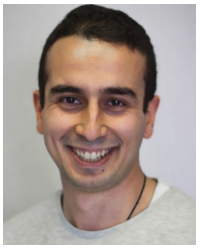

ALIREZA SHAMSOSHOARA received the B.Sc. degree from Shahid Beheshti University (SBU) in 2012, the M.Sc. degree in electrical engineering from the Khaje Nasir Toosi University of Technology (KNTU), Tehran, Iran, in 2014, the M.Sc. degree in informatics from Northern Arizona University, in 2018, and the Ph.D. degree in informatics from Northern Arizona University, in 2021, under the supervision of Dr. Fatemeh Afghah. He worked as a Network Engineer from 2015 to 2017. He also worked as a Staff Post Doctorate Researcher at Northern Arizona University. Currently, he is an AI Engineer with the Volkswagen Group of America (Innovation Center of California). His research area and thesis was about unmanned aerial vehicles and drones for disaster situations such as wildfires. He focused on tools such as reinforcement learning and imitation learning during his Ph.D. His main research interests include autonomous driving, machine learning, and robotics.

SAFIN B. SALIH received the bachelor's degree in mathematics and the master's degree in computer science from Georgia Institute of Technology. During their academic years, he undertook several projects, notably including the development of a eating detection model for wearable technology. Additionally, he gained professional experience in various roles, beginning with a position at Leanardo, a defense company based in Italy. In this role, they contributed to projects involving real-time object detection for vehicles and an optical character recognition (OCR) model for license plate recognition.

PEDRAM AGHAZADEH received the B.S. degree in computer science from the University of Tehran in 2022. From 2019 to 2022, he worked as a Teaching Assistant and an Informatics Olympiad Teacher. Since 2022, he has been with the Volkswagen Innovation and Engineering Center California, as an AI Engineer, where he worked on various projects including AI trajectory planner, vision language models, and bird's eye view mapping. His research interests include reinforcement learning, imitation learning, and multi-modal language models.